Original articles

Theoretical and experimental investigation on ADT organic semiconductor in different solvents

D. M. Mamand[1], H. H. Rasul[1], P. K. Omer[2], H. M. Qadr[1]✉

[1]University of Raparin, College of Science, Department of Physics,
Sulaymaniyah, Iraq

[2]University of Raparin, College of Science, Department of Chemistry,
Sulaymaniyah, Iraq

Abstract

The purpose of this work is to investigate experimental and theoretical methods for the properties of (ADTs) organic semiconductors. The effect of solvent on optical and electrical on Anthradithiophene (ADT) characteristics was investigated. The optoelectronic properties associated with experimental work consists of bandgap energy, Tauc plot, transparency, electrical and optical conductance and dielectric properties calculated. For theoretical calculations, firstly, HOMO and LUMO have been used for the computation of the bandgap energy. The average bandgap energy between HOMO and LUMO is found to be 2.84 eV by using five basis sets in gas phases. After that, the FTIR has been elucidated. In addition, to determine the functional group, and determined the important region did not take place absorption. In general, this region did not occur absorption which is around between 1650 cm^{-1} and 3200 cm^{-1} by using five basis sets. The UV-Vis spectroscopy was elucidated. Furthermore, to determine the energy band-gap, the average energy band gap was found to be 2.59 eV, and it was determined the correct transition type. The ADT molecule exhibited the indirect allowed transition.

Keywords: UV-visible spectroscopy, FTIR, HOMO, LUMO, HF and DFT

✉ Hiwa Mohammad Qadr, e-mail: hiwa.physics@uor.edu.krd

Condensed Matter and Interphases / Конденсированные среды и межфазные границы   2022;24(2): 227–242

D. M. Mamand et al.   Theoretical and experimental investigation on ADT organic semiconductor...

1. Introduction

Organic semiconductors (OS) have been investigated as different to conventional inorganic semiconductors by their low cost and ease of manufacture. Applications envisioned for OS include thin film (TF) transistors, light-emitting diodes (LED), solar cells (SC), and photo-refractive devices. Small molecular of the weight solution-processable materials that can be cast into high-performance conductive that TF has special technical significance [1–6]. Organic TF transistors formed on pentacene or oligothiophenes have reached device performance with mobilities in the range of 0.1–1 cm² V⁻¹ s⁻¹ with large on/ off current ratios [1]. The most important material properties for the semiconductors to create thin film (TF) are high mobility, low "off" conductivity, stability and processability [7, 8].

Anthradithiophene (ADTs) showed better stability than pentacene and was lower than the experimental value by nearly 0.6 eV. The IP of ADT is calculated to be 6.15 eV and the ADT has small reorganization energy of 0.094 eV is equivalent to pentacene [9-17]. Slight chemical modifications of the side groups of both ADT and pentacene derivatives bring about considerable variations in molecular packing which affects electronic and optical properties (OP) of TF [1] . Its single crystal, alerted by H. Katz et al., which have become a common core in both small-molecule semiconductor and polymeric systems [7]. ADTs have produced materials with hole-mobility extracted from field-effect transistor
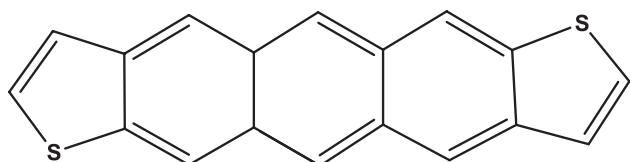

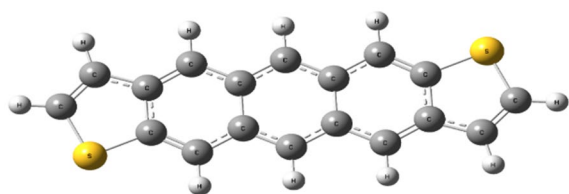**Fig. 1.** Chemical structure of ADT organic semiconductor

Fig. 2. Optimized ADT organic semiconductor

(FET) devices on the order of 0.1 cm² V⁻¹ s⁻¹ [12, 13], but EFT exposed differences mobilities of 0.12 cm² V⁻¹ s⁻¹ for anti-ADT [8]. The hole mobility in ADT single crystals nearly increases with decreasing temperature following a power law ($\mu \propto T-n$) [13, 14].

O. Kwon et al. have studied ADT, the intrinsic electronic structure, the relevant intermolecular interaction, and the intramolecular vibrational modes which are very comparable to those in pentacene [15]. Also, they indicated that the first ionization of Anthra [2, 3-b: 6, 7-b'] dithiophene has an energy of vertical is around 6.6996 eV and the anti-ADT is more stable than the syn-ADT by nearly 0.02 kcal/mole. The angular ADT molecules have the low-lying HOMO level (–4.81 eV), also LUMO level is calculated to be –2.02 eV, the band-gap energy is estimated to be 2.79 eV. The ADT indicates great oxidation stability in organic field-effect transistors (OFET) devices due to the low-lying HOMO level and the implementations of OFETs [16].

Some researchers used the ADT-donor unit and aforesaid acceptor units to synthesize corresponding copolymers to explore their photovoltaic performance. ADT was manufactured as reported earlier. Thin (ten micrometres) sized platelets of ADT single crystals were grown from the vapour phase in a stream of gas [7]. J. Schön et al. [15] have been reported that the properties of the ADT is a small organic molecule and charge transport dependence of temperature, in the layered p-type, the mobility for in-plane transport displays an inverse power law temperature. The ADT was initially synthesized as a mixture of anti-isomer and syn-isomer due to complications with isomer departure [13].

This paper investigates optoelectronic properties in high-quality Anthradithiophene organic material, the chemical structure shown in Fig. 1. Moreover, the influence of molecular structure and energy reflectivity, dielectric constant and bandgap are important for this study.

2. Computational procedures

In performing the theoretical calculations, Gaussian 09 program was used [19]. In the investigation of molecule structure and quantum chemical computational calculations, many

Condensed Matter and Interphases / Конденсированные среды и межфазные границы   2022;24(2): 227–242

D. M. Mamand et al.   Theoretical and experimental investigation on ADT organic semiconductor...

software is possible in the literature depending on the purpose of the work, the optimized molecule structure is shown in Fig. 2. In this study, to explain the theoretical optical properties and structure of the molecule, the electrostatic potential map and UV-visible was used. The first optimized the molecule structure in the various basis set for comparison between them. Based on DFT, the HOMO has the highest occupied molecular orbital and LUMO has the lowest unoccupied molecular orbital which is calculated in various basis sets. According to bandgap energy, the comparison between theoretical and experimental results was performed. The UV-visible spectroscopy, HOMO and LUMO and electrostatic potential map calculations associated with Hartree-Fock and density functional theory were performed to compare the results, according to various basis sets such as Split-Valence Basis Sets (SVBSs) 6-31G and 6-311G. In addition, the single first polarization function is 6-311++ (d,p), the basis set 3-21G has polarization functions on second-row atoms only, and LANL2DZ (Los Alamos National Laboratory 2 double ξ) basis set represents the transition metals electrons.

2.1. Theoretical calculation of ADT molecule properties

This study obtained several properties of the ADT molecule based on the DFT and HF approximations of different basis sets. There are two important parameters which are HOMO and LUMO energy. HOMO is the highest energy-filled molecular orbital, but LUMO is the lowest energy empty molecular orbital. The tendency of molecules to give electrons or to receive electrons can be decided based on Lewis bases. For instance, HOMO means a high-energy molecule in water that has a high tendency to give out electrons, and LUMO means a high-energy molecule in water that has a high tendency to receive electrons [20].

The ionization energy can calculate based on HOMO energy. Thus, the energy was required to break an electron out of a chemical species in the gas phase or the isolated state. Theoretically, using Kopman's theorem, can interpret and estimate the ionization energies of the chemical species which are the energy required to break an electron from HOMO [21, 22]:

$$I = -E_{\text{HOMO}}. \tag{1}$$

In the gas phase or isolated state, the energy change in an electron uptake reaction of a chemical species indicates the electron affinity. The LUMO energy is related to electron affinity considering the electron to be received which will enter the lowest-energy free orbital in a basic type. According to Koopmans theory can calculate the electron affinity A, as the following equation:

$$A = -E_{\text{LUMO}}. \tag{2}$$

The difference between the HOMO and LUMO indicates the bandgap energy and can be expressed as the following:

$$\Delta E = E_{\text{LUMO}} - E_{\text{HOMO}}. \tag{3}$$

The HOMO and LUMO of molecules describe the strong ionic and covalent interaction. A strong covalent chemical interaction is expected between molecules which energy gap is close to each other. Based on the energy gap, some physical and chemical properties of the particles can be determined such as the nonlinear properties and spaced low energy particles which predict to exhibit nonlinear optical properties and exhibit photoconductivity.

Electronegativity, hardness and softness are very significant parameters to investigate the electronic properties of molecular, finite study have been performed on corrosion inhibition efficiency based on these parameters. A soft molecule refers to large and high polarized chemical species, but a hard molecule refers to small and low polarized species:

$$\eta = \frac{I - A}{2}, \tag{4}$$

$$\sigma = \frac{1}{\eta}, \tag{5}$$

where η is the hardness and σ is the softness. Based on DFT, the relationships between ionization energy and electron affinity can calculate the absolute electronegativity or Mulliken electronegativity which is the arithmetic mean of the ionization energy and electron affinity of the species. The power of a molecule to accept and donate the electron depend on the electronegativity of the molecule. More powerful electron acceptors or electrophiles indicates the molecule

Condensed Matter and Interphases / Конденсированные среды и межфазные границы   2022;24(2): 227–242

D. M. Mamand et al.   Theoretical and experimental investigation on ADT organic semiconductor...

which has a high electronegativity. Lower electronegativity indicates the power of the molecule to electron donors or nucleophiles:

$$\chi = \frac{A+I}{2}. \qquad (6)$$

Molar Gibbs free energy and Gibbs free energy for a pure substance can be described by chemical potential. When the Gibbs free energy is low, the activity of the substance will be small. The following expression can calculate the chemical potential:

$$CP = -\chi. \qquad (7)$$

Electrophilicity index ω is another significant molecule property and is a measure of energy reduction due to the maximum electron flow between the transceiver, based on the following equation:

$$\omega = \frac{(CP)^2}{2\eta}. \qquad (8)$$

Electrophilicity index affects the amount of electron flux which species with a high electrophilicity index. According to the definition of the electrophilicity index, species with a high electrophilicity index have more electron flux if they are involved in a transponder interaction and lower the energy more because of this electron flux. The results of the HF approximation calculations have no similarity or approximation with experimental results associated with different solvents as shown in Table 1. The DFT results are close agreement with experimental results as shown in Table 2. The results of the DFT can rely on explanation and investigation of the chemical property of ADT molecules because the bandgap energy difference between them is no more than 1.3 eV, especially in CHF solvent. Both HF and DFT methods are used to solve the quantum states of multi-electron systems such as molecules and crystals, each of them based on the Born–Oppenheimer approximation. The lack of the results of ADT molecule calculations in these basis sets because of the Hartree-Fock method assumes that the many-electron wave function takes the form of a determinant of single-electron wave functions which is called a Slater determinant. The problem with this assumption has a problem to express a single determinant and is that a general many-electron wavefunction cannot be expressed as a single determinant. According to HF approximation, the resulting energies as calculated tend to be too high, and the disadvantaged in Hartree-Fock methods do not fully incorporate electronic correlation. The configuration reaction in this method requires finding a complete basis for the single-electron

Table. 1. Quantum chemical calculation of several properties in different basis sets for ADT molecule according to HF

Basis set	HOMO	LUMO	I	A	ΔE	η	σ	χ	CP	W	μ
6-21G	−6.85	1.16	6.85	−1.16	8.01	4.005	0.249	2.845	−2.84	1.01	0.989
6-31G	−6.697	1.184	6.697	−1.18	7.881	3.94	0.253	2.756	−2.75	0.96	1.03
6-31G (d, p)	−6.503	1.33	6.503	−1.33	7.833	3.91	0.255	2.586	−2.58	0.85	1.17
6-311G	−6.825	1.015	6.825	−1.01	7.84	3.92	0.255	2.905	−2.90	1.07	0.92
LanL2DZ	−6.827	0.893	6.827	−0.89	7.72	3.86	0.259	2.967	−2.96	1.14	0.87
SDD	−6.817	0.915	6.817	−0.91	7.73	3.86	0.25	2.95	−2.95	1.12	0.88

Table. 2. Quantum chemical calculation of several properties in different basis sets for ADT molecule according to DFT

Basis set	HOMO	LUMO	I	A	ΔE	η	σ	χ	CP	W	μ
6-21G	−2.103	−0.672	2.10	0.67	1.43	0.71	1.39	1.38	−1.38	1.345	0.743
6-31G	−4.969	−2.067	4.96	2.06	2.90	1.45	0.68	3.51	−3.51	4.264	0.234
6-31G (d, p)	−4.809	−2.024	4.80	2.02	2.78	1.39	0.71	3.41	−3.41	4.191	0.238
6-311G	−5.189	−2.299	5.18	2.29	2.89	1.44	0.69	3.74	−3.74	4.85	0.206
LanL2DZ	−5.113	−2.284	5.11	2.28	2.829	1.414	0.70	3.69	−3.69	4.835	0.206
SDD	−5.095	−2.271	5.09	2.27	2.824	1.412	0.708	3.68	−3.68	4.803	0.208

Condensed Matter and Interphases / Конденсированные среды и межфазные границы   2022;24(2): 227–242

D. M. Mamand et al.   Theoretical and experimental investigation on ADT organic semiconductor...

wave functions. Then for these wave functions, the exact wave function of many electrons can be expressed as a linear set of all possible determinants. In the density functional theory (DFT), the wave function of many electrons is passed exactly in favour of the electron density associated with the Hohenberg-Kohn Theorems [21, 22]. The DFT mechanism for the total energy related to the ground state energy of the system is uniquely dependent on the electron density and total energy being a function of the electron density. Thus, regarding the electron density, to minimize energy, one can implement the anisotropy principle. It can not know what the energy function is, which is the problem of the DFT method. Keeping track of the spatial and spin coordinates of all N electrons requires in HF calculations. But according to DFT calculations, DFT offers the potential advantage of trading with only a single function of a single spatial coordinate. During this purpose, the applicant of DFT has been regularly growing in prevalence. Fig. 3 shows the visualization of HUMO and LUMO for ADT $C_{18}H_{10}S_2$.
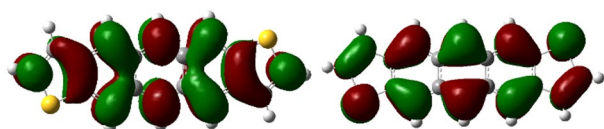
HOMO   LUMO

Fig. 3. The HOMO and LUMO of ADT $C_{18} H_{10} S_2$

3. The FTIR studies of the ADT organic semiconductor for different solvents

The harmonic vibrational frequency of the ADT semiconductor for different basis sets have been calculated based on the HF and DFT. In this study to investigate in depth the functional groups of the molecule, vibrational band assignments were generated using Gauss-View molecular visualization software and compared with the experimental results. Fig. 4 a and b show the correspondence between the theoretical and experimental calculations. The chemical structure of ADT is anthracene which is isoelectronic to pentacene, with five linearly-bonded aromatic rings from C = C-C in benzene rings and C-H ring which is related to vibrations. The presence of one or more aromatic rings in a structure is usually readily determined. The ADT molecular has four bounds as carbon-carbon single bond (C-C), carbon-carbon double bond (C=C), carbon-hydrogen bond (C-H) and carbon-sulfur single bond (C-S) as shown in Table 3. The advantage domain in infrared absorption is to determine the functional groups. There are two types, in which vibrations can take place, for example, bending and stretching. The bending is much lesser for the same bond since there is less resistance.

Fig. 4 b shows the FT-IR spectra of the ADT molecule for dichloromethane (DCM), chloroform (CHF) and Dimethylacetamide (DMAC) solvents. The FT-IR spectrum of the bands at about 2355 cm⁻¹ for these solvents gives a strong peak
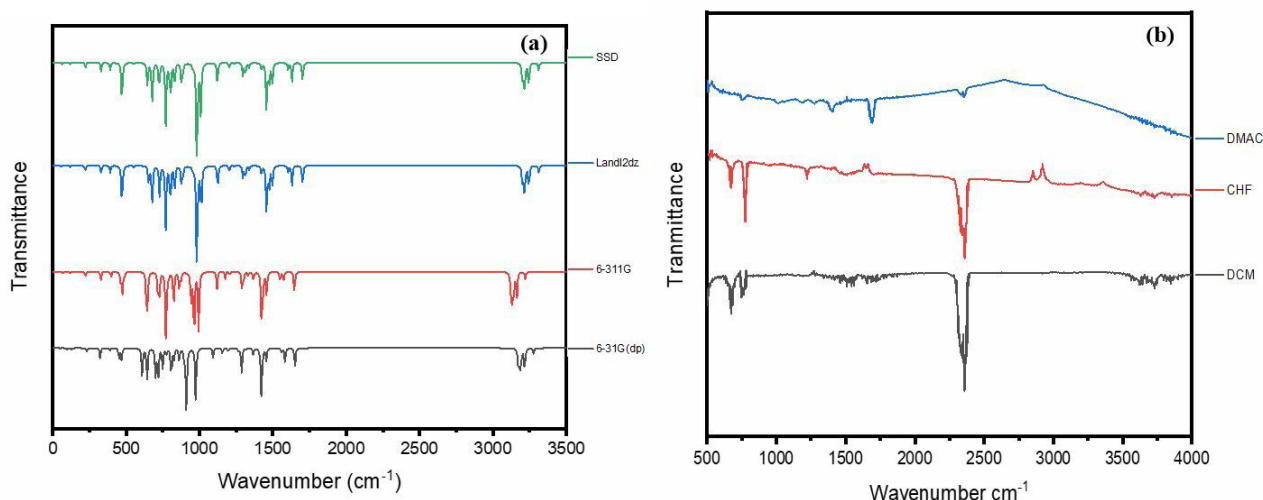
Fig. 4. FTIR absorbance spectra of the ADT organic semiconductor for CHF, DCM and DMAC solvent: (*a*) Theoretical, (*b*) Experimental

Condensed Matter and Interphases / Конденсированные среды и межфазные границы   2022;24(2): 227–242

D. M. Mamand et al.   Theoretical and experimental investigation on ADT organic semiconductor...

Table. 3. Characteristic IR absorption frequencies of organic functional groups

Groups	Absorption (cm⁻¹)	Groups	Absorption (cm⁻¹)
C=C Bending	1700–1500	C-H Bending	1650–2000
C=C Stretched	1400–1600	C-S Stretch	690–685
C-C Stretch in ring	1585–1600	C-H Bending out of the plane	900–675
C-H Stretch	3000–3300	C-H Bending weak overtone	1650–2000

which shows the strong C-H stretching. The IR spectrum band at 1693 cm⁻¹ for DMAC solvent corresponds to hydrogen bonding. The IR spectrum band at 1402 cm⁻¹ for DMAC solvent shows the δC-H$_3$. The IR spectrum band at 1219 cm⁻¹ for CHF solvent indicates the CH$_2$ and CH$_3$ groups. The IR spectrum band at 772 cm⁻¹ for CHF solvent indicates the strong C-C stretching. The IR spectrum band at about 750 cm⁻¹ for CHF and DCM solvents shows the C-H bending. The IR spectrum band at about 668 cm⁻¹ for CHF and DCM solvents shows the C-S stretching.

3.1. UV-visible spectra

Organic semiconductor materials have a wide range of applications and owe their semiconducting properties to the presence of conjugated double bonds in their molecular structure. The hybridization of carbon atoms is sp^2 of conjugated double bonds and causes a rise in π and σ bonds. The energy levels consist of two split regions which have the lower energy level as the highest occupied molecular orbital (HOMO) and the higher energy level as the lowest unoccupied molecular orbital (LUMO) [25–27]. Because of some significant properties, the organic dyes have attracted attention as novel materials in high-density optical data recording media due to their low heat conduction, diversity of optical characteristics and chemical stability. The broad and narrow bandgap energy of the semiconductor are a significant characteristic of fabrication devices. Controlling the particle size and the overall photoactivity can greatly expand the hybrid semiconductor system causing the optical absorbance of narrow-band semiconductors which can incrementally tun to the absorption in the visible region [28].

The bandgap energy of Anthra [2, 3-b: 6, 7-b'] Dithiophene (ADT) molecule calculated is associated with the UV-visible spectrum as shown in Fig. 5a and b for DCM, CHF and DMAC solvents. They investigate the UV-Vis spectra of the ADT molecule for the solvents of DCM, CHF, and DMAC. Absorbance is important for optoelectronic applications. The ADT molecule exhibits the maximum peaks at 296, 297 and 295 nm, respectively. As can be seen from the relevant curves, the ADT molecule dissolved in the DCM solution shows the largest and most stable spectrum. The ADT molecule is much more dominant in the near-ultraviolet region. The bandgap energy of the ADT molecule for CHF solvent is 4.92, 4.17 eV, whereas it is observed 4.9 and 4.18 eV for DCM, and DMAC is 4.2 and 4.59 eV. In the calculation concerning each maximum absorption, the bandgap energies are very close.

The crucial properties of semiconductor material are the absorption of light. There are two terms of absorption coefficient α and $h\nu$ exhibits light absorption. From the following expression can calculate the forbidden bandwidth of optical transitions or optical bandgap of semiconductors E_g [27]:

$$\alpha = \frac{2 \cdot 303 A}{L}. \tag{9}$$

$$k = \frac{\alpha\lambda}{4\pi}. \tag{10}$$

Where α is absorption coefficient, A is absorbance, L is thickness (1 cm in my case).

$$(\alpha h\nu) = A^* (h\nu - E_g)^m. \tag{11}$$

Here, A^* is a constant and m is the parameter related to the measuring type of band gaps. The crystal momentum conservation and energy conservation for any transition to take place have to be satisfied. The bandgap of a semiconductor includes two types which direct and indirect bandgap in semiconductor physics. In the valence band maximal-energy state and the
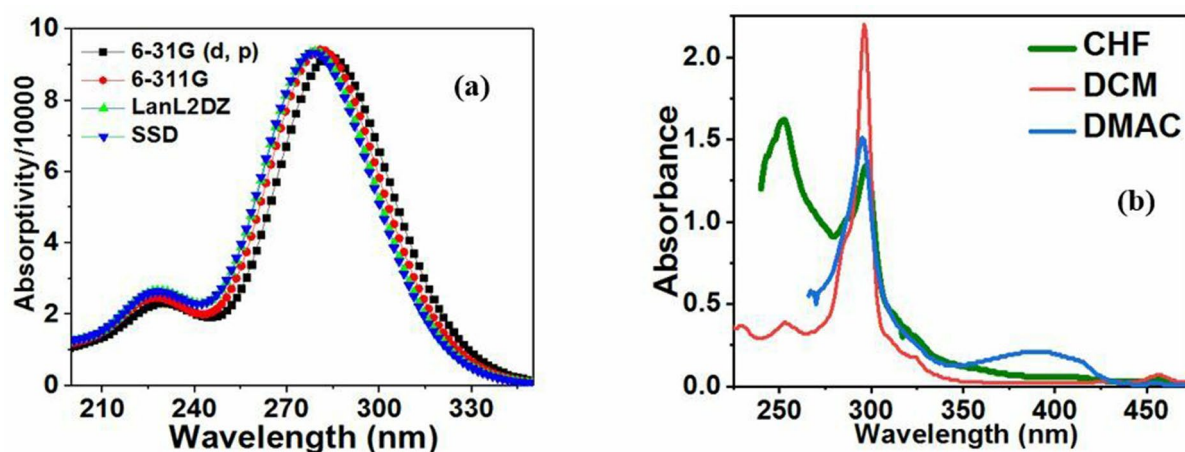
Condensed Matter and Interphases / Конденсированные среды и межфазные границы   2022;24(2): 227–242

D. M. Mamand et al.   Theoretical and experimental investigation on ADT organic semiconductor...

Fig. 5. UV-visible spectra of ADT molecule: (*a*) Theoretical in the various basis set and (*b*) experimental in different solvent

Table 4. Maximum absorption and bandgap energy of ADT in various solvents with the comparison between experimental and theoretical

Experimental	DCM		CHF		DMAC			
λ_{max}, nm	253	296	252	297	265	295		
E_g, eV)	4.92	4.17	4.9	4.18	4.2	4.59		
Theoretical	631G (d. P)		6311G		LanL2DZ		SDD	
λ_{max}, nm	228	284	226.5	280	226	277	228	277.6
E_g, eV)	5.44	4.37	5.48	4.43	5.49	4.49	4.30	4.47

conduction band, the minimal energy state in the Brillouin zone is characteristically identified by a certain crystal momentum. If the crystal momentum of electrons and holes are different in both the conduction band and the valence band which are called the indirect bandgap. The electron momentum of the top of the valence band and the bottom of the conduction band is not always the same. The top of the valence band and the bottom of the bandgap in a direct bandgap semiconductor have the same momentum value. By the comparison between the UV-visible bandgap energy and the Tauc plot, the method obtained the type of bandgap energy of ADT compound is indirect. The value of m is dependent on the type of semiconductor bandgap energy and include four various value which is 3/2 for forbidden transition, 3 for forbidden indirect transition, 2 for allowing indirect transition.

Fig. 6 shows Tauc plot of ADT molecule for three different solvents. The allowed direct bandgap was obtained from the linear region. The optical band gap E_g value for all solvents is 4.058

and 4.07 eV. For CHF solvent, E_g has the same value, but for DAMC g is 4.07 eV. The E_g of semiconductor material is significant to operate the solar cells at this range because the devices can operate at high voltage and temperature. The change of solvents from DAMC to ADT as illustrated in Figures 5 and 6, enables more electrons to enter the conduction band by longer photon wavelengths. When the absorbance increased, the allows more electrons to be conduction band consequently increasing the efficiency of devices.

3.2. Refractive index

In recent decades, the application of semiconductor materials has been attracted to optical designers due to their use in the fabrication of electronic, optoelectronic and optoelectronic properties such as photodetectors (PD), heterogeneous lasers, light-emitting diodes (LEDs), and photonic modulators that operate in regions of Mid-infrared (2–5 µm) and integrated circuits. The refractive index and bandgap energy are two main important properties of semiconductor ma-
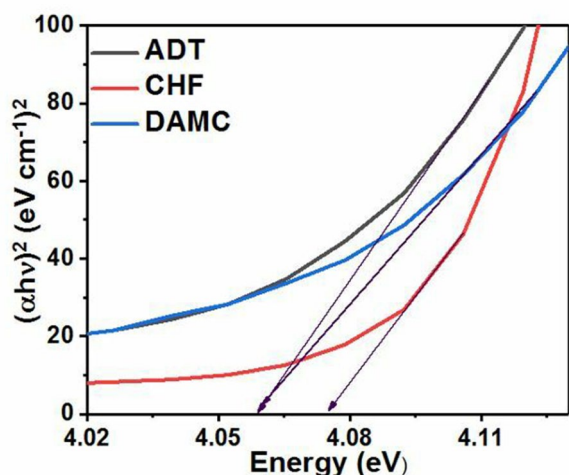
Condensed Matter and Interphases / Конденсированные среды и межфазные границы   2022;24(2): 227–242

D. M. Mamand et al.   Theoretical and experimental investigation on ADT organic semiconductor...

Fig. 6. Tauc plot of ADT molecule for various solvent

Fig. 7. Refractive index against energy bandgap of ADT molecule in various solvent

terials, and the fundamental properties can decide on these two properties [30, 31]. The refractive index is related to the structure of materials and is a measure of transparency to the incident photon. The threshold of photon absorption of a semiconductor determines the energy gap.

The following equation can calculate the refractive index. Fig. 7 shows that the refractive index decreased with increased bandgap energy. The refractive index of ADT molecule in DMAC solvent has the highest value at the lowest Eg after 2.55 eV decreased up to 2.67 eV and interpreted the ADT solvent line of refractive index. Fig. 8 illustrates the effect of solvent in the refractive index of the ADT material. The refractive index of ADT for DMAC solvent at low E_g differs from other solvents, but after 2.67 eV is similar to another solvent:

$$n = \left\{ \left[\frac{4R}{(R-1)^2} - k^2 \right]^{\frac{1}{2}} - \frac{R+1}{R-1} \right\}. \qquad (12)$$

The refractive index of semiconductor material can determine by using many relations such as Ravindra, Moss, Kumar and Singh, Herve and Vandame. These relations depend on bandgap energy, and these relations are extensively used to determine the n of semiconductors [32]:

Reddy relation:

$$n^4 (E_g - 0.365) = 154. \qquad (13)$$

Moss relationship:
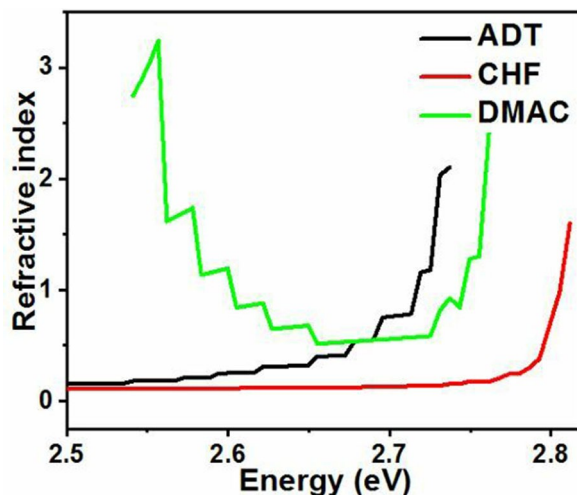
$$n^4 E_g = 95 \text{ eV}. \qquad (14)$$

Kumar and Singh relation:

$$n = KE_g^c. \qquad (15)$$

Where K and C are constants and K is 3.3668 and C is −0.32234.

Herve-Vandamme relationship:

$$n^2 = 1 + \left(\frac{A}{E_g + B} \right)^2 \qquad (16)$$

Ravindra relationship:

$$n = 4.084 - 0.62 E_g. \qquad (17)$$

3.3. Transmittance

The optical transmission spectra for ADT of different solvents are shown in Fig. 9. The transmission spectra at low E_g is high and depends on the type of solvent. The solvent DCM and DMAC at the lowest level have the highest transmission. But for the CHF solvent, the light transmission in the UV visible range is low, compared to other solvents.

The transparent material has poor electrical conductivity and high reflectivity. The ADT molecule at the 3.75 eV for all solvents exhibits the lowest transparency and highest reflectivity. Generally, the transmittance gradually decreases by increasing bandgap energy.

3.4. Normal dispersion region

For investigating the physical properties of materials such as light bending and how light bends at each specific wavelength, should consider the dispersion parameter. Designers
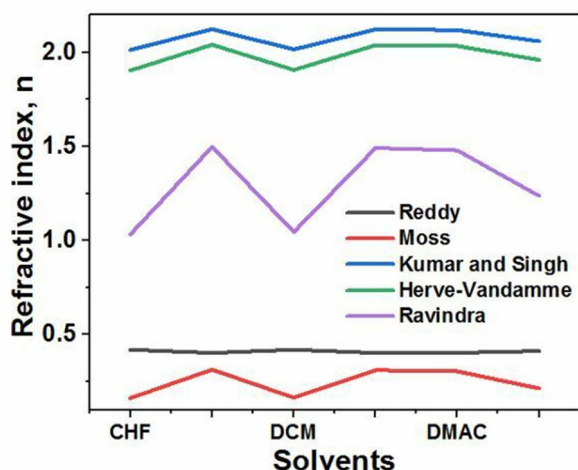
Condensed Matter and Interphases / Конденсированные среды и межфазные границы   2022;24(2): 227–242

D. M. Mamand et al.   Theoretical and experimental investigation on ADT organic semiconductor...

Fig. 8. The refractive index plots of the ADT semiconductor for the various solvents

Fig. 9. Eg against transmittance of ADT semiconductor for various solvents

make materials into optical pigments, and the scattering area is an important property. The scattering area depends on the refractive index of the material. When the angular frequency increases, the refractive index can fluctuate and then increase the scattering area.

In the construction of optical instruments, material dispersion can be a desirable or undesirable effect in optical applications. Allowing more accurate discrimination of wavelengths when using light scattering by glass prisms to create spectroradiometers, spectrometers and stereo grids. The frequency change with the refractive index is called dispersion. The refractive of light decreases at a lower frequency. The angular frequency band of ADT in the CHF solvent has the highest band, and the normal scattering area is 5.6 PHz. In the DMAC solvent, the frequency range is the lowest, and the scattering region is 4.51 PHz. The normal scattering region is 5.4 PHz for ADT molecule in DMAC solvent as shown in Fig. 10.

3.5. Reflectivity and reflection loss

The optical response of the surface of a material can be estimated using the reflectivity coefficient. Reflectivity coefficient is the ratio of the reflected power to the incident power which is important for the optical properties of materials. The relation between the extinction coefficient and refractive index can calculate the reflectivity as the following expression [33, 34].
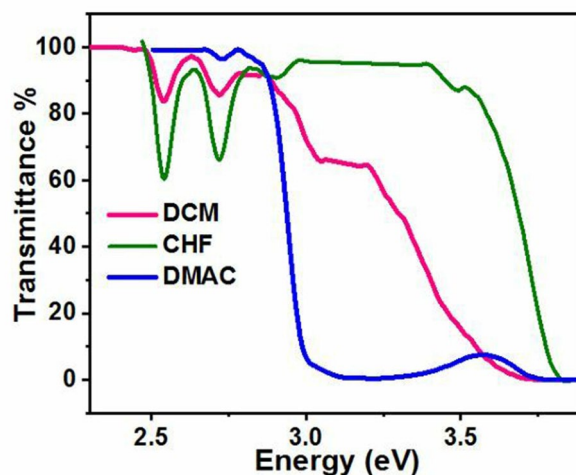
$$R = \frac{(n-1)^2 + k^2}{(n+1)^2 + k^2}, \tag{18}$$

where k is the frequency-dependent extinction coefficient calculated from equation (10), for a weak absorber k can be considered too small and at the high frequency it vanishes. The following expression can calculate the reflectivity at a higher frequency:

$$R = \left(\frac{n-1}{n+1}\right)^2, \tag{19}$$

where n is a refractive index, obtained in equation (12).

The relation between reflectivity and reflection coefficient can determine the reflection coefficient according to the following equation:

$$r = \sqrt{R}. \tag{20}$$

The absorption technique is a significant property, because of the relation between electrical and optical properties through the conductivity tensor. Good electrical conductor material indicates a high reflection, but the transparent materials are expected reasonably poor electrical conductivity. The reflectivity of the ADT molecule associated with the UV visible spectra is well-matched with each other, since the reflectivity ratio depends on the bandgap energy, a large bandgap indicates low reflectance, while a small bandgap indicates high reflectivity as shown in Fig. 11.
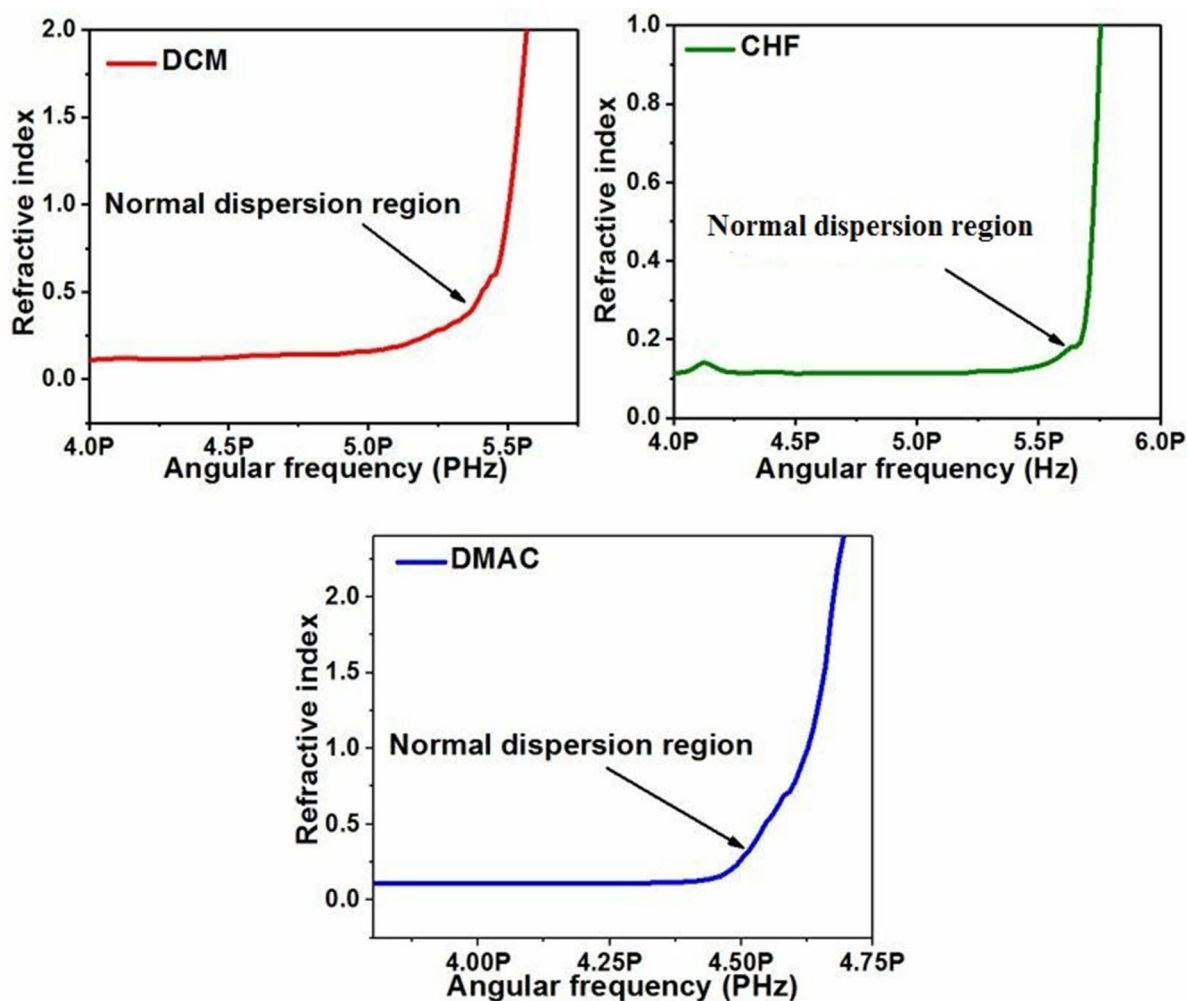
Condensed Matter and Interphases / Конденсированные среды и межфазные границы   2022;24(2): 227–242

D. M. Mamand et al.   Theoretical and experimental investigation on ADT organic semiconductor...

Fig. 10. Normal dispersion region calculation and plot the angular frequency against refractive index of ADT molecule

3.6. Reflection loss and transmission coefficient

The reflection loss and transmission coefficient in telecommunication are the principal characteristics. From the following equations can calculate each of them and the express presents the correlation between the reflection loss and transmission coefficient as shown in Fig. 12. It can be shown that a partial inverse proportionality between the two quantities [34, 35]:

$$R_L = \left[\frac{n-1}{n+1}\right]^2. \tag{21}$$

$$T = \frac{2n}{n^2+1}. \tag{22}$$

For estimates of how much of an electromagnetic wave (light) passes through a surface or an optical element can use the transmission coefficient in the optics field. Using the transmission coefficient, the amplitude and intensity of the wave can be measured. The chemistry field can describe the transmission coefficient to a chemical reaction overcoming a potential barrier [36].

4. Electrical and optical conductivity

There are two important parameters to decide on electrical and optical behaviour which are electrical and optical conductivity based on the following parameters [36].

$$\sigma_{opt} = \frac{\alpha n c}{4\pi}. \tag{23}$$

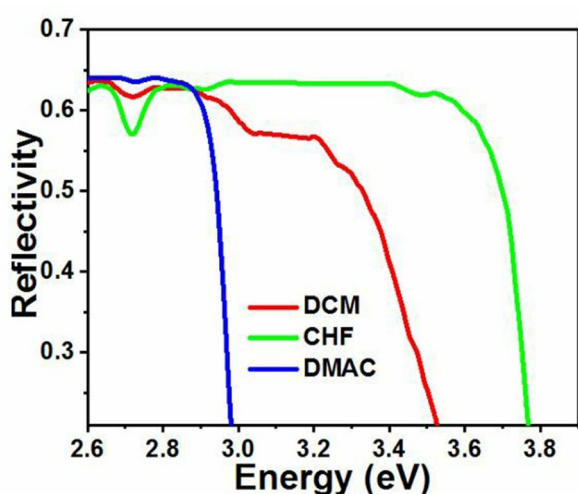$$\sigma_{ele} = \frac{2\lambda\sigma_{opt}}{\alpha}. \tag{24}$$

Condensed Matter and Interphases / Конденсированные среды и межфазные границы   2022;24(2): 227–242

D. M. Mamand et al.   Theoretical and experimental investigation on ADT organic semiconductor...

Fig. 11. Reflectivity relation of ADT molecule with energy gap in various solvent

By considering the electronic structure of materials, due to free electrons in the conduction band, the electrical conductivity of materials and semiconductor optical conductivity are the change in conductivity induced by illumination, both a decrease or an increase.

The Drude model explained the electrical conductivity of materials, and the band theory plays a significant role in explaining the concept of conductivity. The conduction band get more free electrons when the valence band and conduction band overlapped. The resistivity possesses in the material, and the scattering mechanism describes the process, and the excited electrons from the valence band to the conduction band are responsible for conduction. The dielectric constant of a material is related in this process to allowing light to propagate through the material. In the case of optical propagation, the relaxation time and plasma frequency are important [37]. Two physical quantities are playing an important role because when light energy as a photon hits the surface of the material, it drives the electron. If there is no scattering, the light gets reflected totally, and hence metals are shiny. This part is associated with the material colour.

The electrical conductance of the ADT molecule differs in various solvents. The electrical conductivity in the range 2.87 to 3.4 eV have the highest value which indicates the ADT molecule easily allows electric current to flow through it for DMAC solvent, and inversely. Electrical resistivity measures how strongly a material
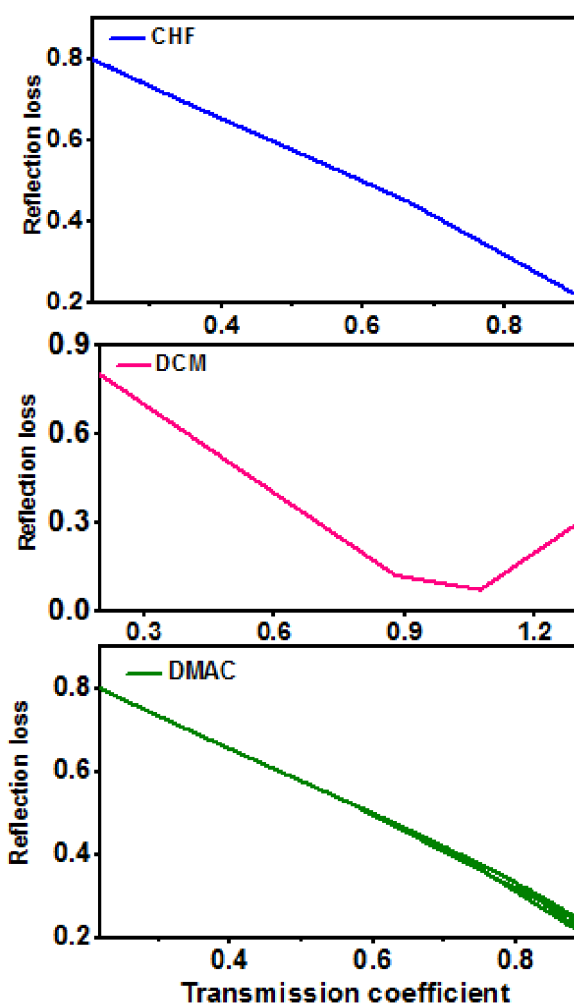

Fig. 12. Transmission coefficients against reflection loss of ADT molecule for different solvents

resists the flow of electric current. In the CHF solvent, the electrical conductivity is the lowest at 3.78 V and then has risen slightly. At the small bandgap energy, the ADT molecule in CHF solvent is not allowed the electric current to through it. Generally, the electrical conductance for each solvent rises after 3.6 eV which indicates the ADT molecule and has a wide range of bandgap energy. The type of solvent is very significant to the optoelectronic and electrical properties of molecules. The optical conductance has lower than the electrical conductance of the ADT molecule, as shown in figure 13b. The electrical and optical conductance have more similarity based on Figures 13 a and b. It can be clearly seen that energy increases and then decreases, after that both are the same according to the bandgap energy of various solvents. The

Condensed Matter and Interphases / Конденсированные среды и межфазные границы   2022;24(2): 227–242

D. M. Mamand et al.   Theoretical and experimental investigation on ADT organic semiconductor...

optical conductivity at the high energy gap has a high value, and the lines are more increased compared with electrical conductance. The wide bandgap and increasing optical conductance at 3.6 eV indicates the ADT molecule which has a wide bandgap and is very useful to fabrication for materials operating at high voltage and temperature such as solar cells. The increase of σ_{real} and $\sigma_{optical}$ can be attributed to an increase in the absorption coefficient in this region. Whereas, a decrease of σ_{real} value after the second peak can be attributed to a decrease in the absorption coefficient within this energy region. These two peaks of the ADT molecule in DMAC in the σ_{real} show areas of deeper penetration for electromagnetic waves, and they also show high conductivity. When the photons are at these peak energy values, the high conductivity can be optimized.

4.1. Dielectric constant

For investigation about the conduction properties of materials, the dielectric constant is a significant parameter. The usage of the film for photovoltaic applications depends on the electrical properties of the materials which are a great importance in determining the usage. The various growth parameters related to the electrical properties such as rate of deposition and substrate temperature [38]. The two parameters ε' and ε'' represent the real part dielectric constant and imaginary part (dielectric loss), respectively. The complex dielectric constant can calculate from the following expression:

$$\varepsilon^* = \varepsilon' + j\varepsilon'', \tag{25}$$

where ε' is represent the real part of dielectric constant, ε'' is represent the dielectric loss and the complex dielectric constant is ε^*. The dielectric spectroscopy of materials is very important because it is related to many parameters such as grain boundary, grain and insights into the structure of compounds, transport properties and charge storage capabilities of dielectric material. At the grain boundaries, potential barrier generates in the thin films or solids which cause the increase of dielectric constant with increasing frequency and is related to the presence of space charge polarization [39, 40].

The polarization concepts of ADT molecules in various solvents can rely on the relation between the dielectric loss and permittivity modalities because polarization depends on the electric field under the condition. If the relaxation time of the electric field applied and frequency is the same which indicates the occurring phase lag. On the other hand, when the frequency is slower than the relaxation of the electric field, polarization occurs. Depolarization does not occur when the relaxation time is lower than the frequency of the electric field. Fig. 14 shows the frequency variation with the real and imaginary part of the dielectric constant of ADT for different solvents.

4.2. Electrostatic potential map

This section describes a map that is called an electrostatic potential map (often called a potential map). It explains information about atomic charges which can suggest advantages of EPM [41]. The first is used for specifying the polar and nonpolar on the parts of the molecule. The second advantage can be used to compare
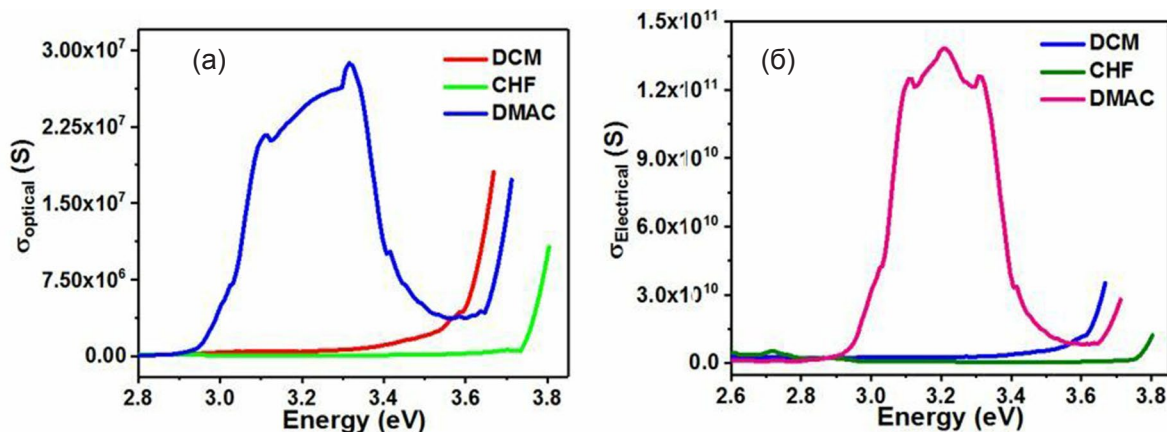

Fig. 13. Variation of optical (*a*) and electrical (*b*) conductivity of ADT molecule

Condensed Matter and Interphases / Конденсированные среды и межфазные границы   2022;24(2): 227–242

D. M. Mamand et al.   Theoretical and experimental investigation on ADT organic semiconductor...

the charges between one molecule with another to obtain information about the product of a chemical reaction. The third factor investigates the shape of the electron cloud of atoms and reveals an irregularity used to tell which region has the highest electron density or concentration and which area has the lowest electron density or depletion. The final advantage, according to this study is to determine which charge atoms repel or attract to the molecules. The interaction between molecules is similar to why molecules assemble and how polymer complexes are formed. These reactions are also related to a chemical reaction. The electrostatic potential map is the actual valuable three-dimensional chart of molecules. It is useful for explaining the charge distribution of charges on the surface of the molecule and investigating the properties of molecules. They permit the researcher to imagine the form and size of the molecule [42]. The electrostatic potential has very powerful for predicting the behaviour of complex molecules. Colour codes to identify charge distribution [43]. The default colour scale starts from the red area to the darker blue. The red colour tells us that the region has a higher electron density, which means that the electrostatic potential has decreased and is at its lowest. This means that the red area in Fig. 15 indicates the largest region of electronegativity. Moreover, the blue colour represents a small electronegativity. Associate with yellow and green, they have more electronegativity than blue, less than red. Yellow is more electronegative than

green. Recall that the area of lowest electrostatic potential corresponds to the region of greatest electron concentration. Around sulfur have more electronegativity comparing with another area. As well as, around of all hydrogens have less electronegativity compared with other regions. The sulfurs have the highest electronegativity value, and the hydrogens have the smallest electronegativity value. On the other hand, the sulfur would be affiliated with the red region of the EPM, and the hydrogen would be affiliated with the blue area. The sulfur has 6 valence electrons and is involved in forming chemical bonds with other elements, and hydrogen has one valence electron.

5. Conclusion

In this investigation, the optical and electrical properties of ADT molecule organic semiconductors for different solvents with theoretical and experimental methods were compared in detail. From the UV-visible spectroscopy calculated the optoelectronic properties such as bandgap energy, allowing indirect transition, refractive index, angular dispersion region, electrical and optical conductivity and dielectric properties in various solvents. The bandgap energy is condensed and determined in many ways to explain the optoelectronic properties. The experimental results in the various basis set are a good agreement with theoretical results. DFT and HF approximation are two significant theoretical methods. The calculations based on them were
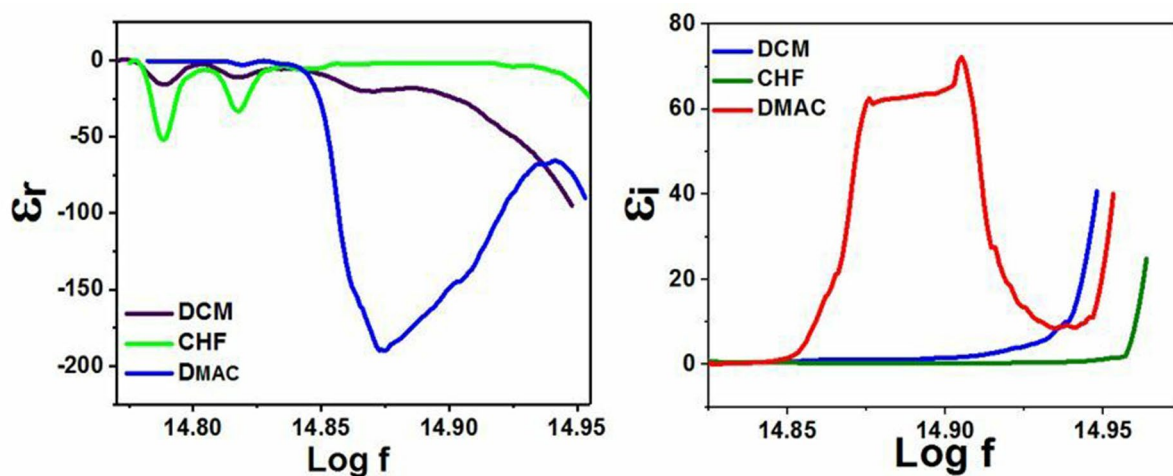

Fig. 14. Relation between the real and imaginary part of the dielectric constant of ADT molecule in three different solvents

Condensed Matter and Interphases / Конденсированные среды и межфазные границы   2022;24(2): 227–242

D. M. Mamand et al.   Theoretical and experimental investigation on ADT organic semiconductor…
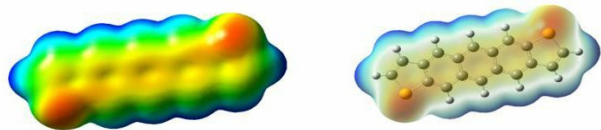

Fig. 15. The Potential Energy Surfaces (PES) of ADT molecule

performed and compared the results for the ADT molecule. The average band-gap energy between the HOMO and LUMO was found to be 2.84 eV by using five basis sets. As a result, based on DFT techniques along with B3LYP, some basis sets were utilized for optimizing the ADT. The result was shown that the electrostatic potential map (EPM) of ADT in the sulfurs have the highest electronegativity value and the hydrogens have the lowest electronegativity value. In this study, the advantages of ADT investigated optoelectronic characteristics of the ADT for various methods and conditions will provide to optoelectronic technologies due to interesting and significant results.

Author contributions

All authors made an equivalent contribution to the preparation of the publication.

Conflicts of interest:

The authors state that there is no conflict of interest in the printing of this manuscript.

References

1. Platt A. D., Day J., Subramanian S., Anthony J. E., Ostroverkhova O. 'Optical, fluorescent, and (photo) conductive properties of high-performance functionalized pentacene and anthradithiophene derivatives. *The Journal of Physical Chemistry C*. 2009;113(31): 14006–14014. https://doi.org/10.1021/jp904021p

2. Sekar A., Sivula K. Organic semiconductors as photoanodes for solar-driven photoelectrochemical fuel production.*CHIMIA International Journal for Chemistry*. 2021;75(3): 169–179. https://doi.org/10.2533/chimia.2021.169

3. Li H., Brédas J.-L. Developing molecular-level models for organic field-effect transistors. *National Science Review*. 2021;8(4): nwaa167. https://doi.org/10.1093/nsr/nwaa167

4. Rojas H. C., Bellani S., Fumagalli F., Tullii G., Leonardi S., Mayer M. T., Schreier M., Grätzel M., Lanzani G., Di Fonzo F. Polymer-based photocathodes with a solution-processable cuprous iodide anode layer and a polyethyleneimine protective coating.

Energy & Environmental Science. 2016;9(12): 3710–3723. https://doi.org/10.1039/c6ee01655c

5. Qadr H. M. A molecular dynamics calculation to cascade damage processes. *The Annals of "Dunarea de Jos" University of Galati. Fascicle IX, Metallurgy and Materials Science*. 2020;43(4): 13–16. https://doi.org/10.35219/mms.2020.4.02

6. Qadr H. M. A molecular dynamics study of temperature dependence of the primary state of cascade damage processes. *Russian Journal of Non-Ferrous Metals*. 2021;62(5): 561–567. https://doi.org/10.3103/s1067821221050096

7. Laquindanum J. G., Katz H. E., Lovinger A. J. Synthesis, morphology, and field-effect mobility of anthradithiophenes. *Journal of the American Chemical Society*. 1998;120(4): 664–672. https://doi.org/10.1021/ja9728381

8. Zhu G., Sun Y., Li M., Tao C., Zhang X., Yang H., Guo L., Lin. Ionic crosslinked polymer as protective layer in electrochromic supercapacitors for improved electrochemical stability and ion transmission performance. *Electrochimica Acta*. 2021;365: 137373. https://doi.org/10.1016/j.electacta.2020.137373

9. Qadr H. M. Effect of ion irradiation on the mechanical properties of high and low copper. *Atom Indonesia*. 2020;46(1): 47–51. https://doi.org/10.17146/aij.2020.923

10. Mamada M., Minamiki T., Katagiri H., Tokito S. Synthesis, physical properties, and field-effect mobility of isomerically pure syn-/anti-anthradithiophene derivatives. *Organic Letters*. 2012;14(16): 4062–4065. https://doi.org/10.1021/ol301626u

11. Miao Q. (Ed.). *Polycyclic arenes and heteroarenes: synthesis, properties, and applications*. John Wiley & Sons; 2015. https://doi.org/10.1002/9783527689545

12. Brédas J.-L., Calbert J. P., da Silva Filho D. A, Cornil J. Organic semiconductors: A theoretical characterization of the basic parameters governing charge transport. *Proceedings of the National Academy of Sciences*. 2002;99(9): 5804–5809. https://doi.org/10.1073/pnas.092143399

13. Hallani R. K., Thorley K. J., Mei Y., Parkin S. R., Jurchescu O. D., Anthony J. E. Structural and electronic properties of crystalline, isomerically pure anthradithiophene derivatives. *Advanced Functional Materials*. 2016;26(14): 2341–2348. https://doi.org/10.1002/adfm.201502440

14. Mamada M., Katagiri H., Mizukami M., Honda K., Minamiki T., Teraoka R., Uemura T., Tokito S. Syn-/anti-anthradithiophene derivative isomer effects on semiconducting properties. *ACS Applied Materials & Interfaces*. 2013;5(19): 9670–9677. https://doi.org/10.1021/am4027136

15. Schön J., Kloc C., Siegrist T., Laquindanum J., Katz H. Charge transport in anthradithiophene single

Condensed Matter and Interphases / Конденсированные среды и межфазные границы   2022;24(2): 227–242

D. M. Mamand et al.   Theoretical and experimental investigation on ADT organic semiconductor...

crystals. *Organic Electronics*. 2001;2: 165–169. https://doi.org/10.1016/s1566-1199(01)00022-2

16. Qadr H. M. ʻPressure effects on stopping power of alpha particles in argon gas. *Physics of Particles and Nuclei Letters*. 2021;18(2): 185–189. https://doi.org/10.1134/s1547477121020151

17. Kwon O., Coropceanu V., Gruhn N., Durivage J., Laquindanum J., Katz H., Cornil J., Brédas J.-L. Characterization of the molecular parameters determining charge transport in anthradithiophene. *The Journal of Chemical Physics*. 2004;120(17): 8186–8194. https://doi.org/10.1063/1.1689636

18. Yang H., Locklin J., Singh B., Bao Z. Organic field-effect transistors with solution-processible thiophene/phenylene based-oligomer derivative films. *Organic Field-Effect Transistors VI, International Society for Optics and Photonics*. 2007: 66581A. https://doi.org/10.1117/12.733953

19. Caricato M., Frisch M. J., Hiscocks J., Frisch M. J. *Gaussian 09: IOps Reference, Citeseer*. 2009.

20. Qadr H. M., Mamand D. M. Molecular structure and density functional theory investigation corrosion inhibitors of some oxadiazoles. *Journal of Bio-and Tribo-Corrosion*. 2021;7(4): 1–8. https://doi.org/10.1007/s40735-021-00566-9

21. Mamand D. Determination the band gap energy of poly benzimidazobenzophenanthroline and comparison between HF and DFT for three different basis sets. *Journal of Physical Chemistry and Functional Materials*. 2019;2(1): 32–36. Режим доступа: https://dergipark.org.tr/en/pub/jphcfum/issue/45047/589803

22. Mamand D. M., Qadr H. M. Comprehensive spectroscopic and optoelectronic properties of BBL organic semiconductor. *Protection of Metals and Physical Chemistry of Surfaces*. 2021;57(5): 943–953. https://doi.org/10.1134/s207020512105018x

23. Görling A. Density-functional theory beyond the Hohenberg-Kohn theorem. *Physical Review A*. 1999;59(5): 3359. https://doi.org/10.1103/physreva.59.3359

24. Gilbert T. L. Hohenberg-Kohn theorem for nonlocal external potentials. *Physical Review B*. 1975;12(6): 2111. https://doi.org/10.1103/physrevb.12.2111

25. Mamand D. Theoretical calculations and spectroscopic analysis of gaussian computational examination-NMR, FTIR, UV-Visible, MEP on 2, 4, 6-Nitrophenol. *Journal of Physical Chemistry and Functional Materials*. 2019;2(2): 77–86. Режим доступа: https://dergipark.org.tr/en/pub/jphcfum/issue/50562/645745

26. Iliev V., Tomova D., Rakovsky S., Eliyas A., Puma G. L. Enhancement of photocatalytic oxidation of oxalic acid by gold modified WO_3/TiO_2 photocatalysts under UV and visible light irradiation. *Journal of Molecular Catalysis A: Chemical*. 2010;327(1-2): 51–57. https://doi.org/10.1016/j.molcata.2010.05.012

27. Aceto M., Agostino A., Fenoglio G., Idone A., Gulmini M., Picollo M., Ricciardi P., Delaney J. K. Characterisation of colourants on illuminated manuscripts by portable fibre optic UV-visible-NIR reflectance spectrophotometry. *Analytical Methods*. 2014;6(5): 1488–1500. https://doi.org/10.1039/c3ay41904e

28. Wu J., Walukiewicz W., Shan W., Yu K., Ager W. J., Haller E.E., Lu H., Schaff W. J. Effects of the narrow band gap on the properties of InN. *Physical Review B*. 2002;66(20): 201403. https://doi.org/10.1103/physrevb.66.201403

29. Orek C., Gündüz B., Kaygili O., Bulut N. Electronic, optical, and spectroscopic analysis of TBADN organic semiconductor: Experiment and theory. *Chemical Physics Letters*. 2017;678: 130–138. https://doi.org/10.1016/j.cplett.2017.04.050

30. Herve P., Vandamme L. K. J. General relation between refractive index and energy gap in semiconductors. *Infrared physics & technology*. 1994;35(4): 609–615. https://doi.org/10.1016/1350-4495(94)90026-4

31. Hader J., Moloney J., Koch S. Microscopic theory of gain, absorption, and refractive index in semiconductor laser materials-influence of conduction-band nonparabolicity and coulomb-induced intersubband coupling. *IEEE Journal of Quantum Electronics*. 1999;35(12): 1878–1886. https://doi.org/10.1109/3.806602

32. Ravindra N., Ganapathy P., Choi J. Energy gap–refractive index relations in semiconductors–An overview. *Infrared Physics & Technology*. 2007;50(1): 21–29. https://doi.org/10.1016/j.infrared.2006.04.001

33. Linda D., Duclère J.-R., Hayakawa T., Dutreilh-Colas M., Cardinal T., Mirgorodsky A., Kabadou A., Thomas P. Optical properties of tellurite glasses elaborated within the $TeO_2-Tl_2O-Ag_2O$ and $TeO_2-ZnO-Ag_2O$ ternary systems. *Journal of Alloys and Compounds*. 2013;561: 151–160. https://doi.org/10.1016/j.jallcom.2013.01.172

34. Umar S., Halimah M., Chan K., Latif A. Polarizability, optical basicity and electric susceptibility of Er^{3+} doped silicate borotellurite glasses. *Journal of Non-Crystalline Solids*. 2017;471: 101–109. https://doi.org/10.1016/j.jnoncrysol.2017.05.018

35. Maheshvaran K., Linganna K., Marimuthu K. Composition dependent structural and optical properties of Sm^{3+} doped boro-tellurite glasses. *Journal of Luminescence*. 2011;131(12): 2746–2753. https://doi.org/10.1016/j.jlumin.2011.06.047

36. Yoshino K., Oyama S., Yoneta M. Structural, optical and electrical characterization of undoped ZnMgO film grown by spray pyrolysis method. *Journal of Materials Science: Materials in Electronics*. 2008;19(2): 203–209. https://doi.org/10.1007/s10854-007-9333-2

37. Jiménez-González A. E, Soto Urueta J. A., Suárez-Parra R. Optical and electrical characteristics

Condensed Matter and Interphases / Конденсированные среды и межфазные границы   2022;24(2): 227–242

D. M. Mamand et al.   Theoretical and experimental investigation on ADT organic semiconductor...

of aluminum-doped ZnO thin films prepared by solgel technique. *Journal of Crystal Growth*. 1998;192(3-4): 430–438. https://doi.org/10.1016/s0022-0248(98)00422-9

38. Sassi M., Oueslati A., Moutia N., Khirouni K., Gargouri M. A study of optical absorption and dielectric properties in lithium chromium diphosphate compound. *Ionics*. 2017;2394): 847–855. https://doi.org/10.1007/s11581-016-1903-y

39. Xie P., Wang Z., Zhang Z., Fan R., Cheng C., Liu H., Liu Y., Li T., Yan C., Wang N. Silica microsphere templated self-assembly of a three-dimensional carbon network with stable radio-frequency negative permittivity and low dielectric loss. *Journal of Materials Chemistry C*. 2018;6(19): 5239–5249. https://doi.org/10.1039/c7tc05911f

40. Yang K., Huang X., Huang Y., Xie L., Jiang P. Fluoro-polymer@ $BaTiO_3$ hybrid nanoparticles prepared via RAFT polymerization: toward ferroelectric polymer nanocomposites with high dielectric constant and low dielectric loss for energy storage application. *Chemistry of Materials*. 2013;25(11): 2327–2338. https://doi.org/10.1021/cm4010486

41. Leboeuf M., Köster A., Salahub D. Approximation of the molecular electrostatic potential in a gaussian density functional method. T*heoretical Chemistry Accounts*. 1997;96(1): 23–30. https://doi.org/10.1007/s002140050199

42. Ramalingam S., Babu P. D. S., Periandy S., Fereyduni E. Vibrational investigation, molecular orbital studies and molecular electrostatic potential map analysis on 3-chlorobenzoic acid using hybrid computational calculations. *Spectrochimica Acta Part A: Molecular and Biomolecular Spectroscopy*. 2011;84(1): 210–220. https://doi.org/10.1016/j.saa.2011.09.030

43. Ramalingam S., Karabacak M., Periandy S., Puviarasan N., Tanuja D. Spectroscopic (infrared, Raman, UV and NMR) analysis, Gaussian hybrid computational investigation (MEP maps/HOMO and LUMO) on cyclohexanone oxime. *Spectrochimica Acta Part A: Molecular and Biomolecular Spectroscopy*. 2012;96: 207–220. https://doi.org/10.1016/j.saa.2012.03.090

Information about authors

Dyari Mustafa Mamand, MSc in Atomic and Molecular Physics, Department of Physics, University of Raparin, (Sulaymaniyah, Iraq).

https://orcid.org/0000-0002-1215-7094
dyari.mustafa@uor.edu.krd

Hazhar Hamad Rasul, MSc in Atomic and Molecular Physics, Department of Physics, University of Raparin, (Sulaymaniyah, Iraq).

hazharhrm@uor.edu.krd

Peshang Khdir Omer, MSc in Chemistry, Department of Chemistry, University of Raparin, (Sulaymaniyah, Iraq).

peshang.khdir@uor.edu.krd

Hiwa Mohammad Qadr, MSc in Physics, Lecture of the Department of Physics, University of Raparin, (Sulaymaniyah, Iraq).

https://orcid.org/0000-0001-5585-3260
hiwa.physics@uor.edu.krd